Temporal Structure of Attosecond Pulses from Intense Laser-Atom Interactions

A. Pukhov,[1] S. Gordienko,[1,2] and T. Baeva[1]

[1]*Institut für Theoretische Physik I, Heinrich-Heine-Universität Düsseldorf, D-40225, Germany*

[2]*L.D. Landau Institute for Theoretical Physics, Moscow, Russia*

(Received 31 March 2003; published 22 October 2003)

We find that the high harmonics have a power-law spectrum $I_\omega \sim \omega^{-3.3\pm0.25}$ in a wide frequency domain starting at the ionization potential I_p and down to the plateau beginning. Our spectrotemporal analysis of the emitted radiation displays clear bowlike structures in the (t, ω) plane. These "bows" correspond to Corkum's reencounters of the freed electron with the atom. We find that the bows are not filled and thus cannot be due to any bremsstrahlung. Rather, it is a resonant process that we call *stimulated recombination* (SR). It occurs when an electron with momentum p reencounters the incompletely ionized atom, and interferes with itself still remaining in the ground state. The SR leads to a highly efficient resonant emission at $\hbar\omega = p^2/2m + I_p$ in the form of attosecond pulses. The SR relies on a low level of ionization and strongly benefits from the use of few-cycle laser pulses.

DOI: 10.1103/PhysRevLett.91.173002 PACS numbers: 32.80.Rm, 42.50.Hz, 42.65.Ky

The continuing progress in the technology of ultrashort pulse lasers has led to the landmark breakthrough and to the birth of attosecond physics [1–6]. Attosecond pulses of x rays are produced when intense sub-10 fs laser pulses interact with gases. The mechanism for generation of attosecond pulses (ASP) is closely related to that of high harmonics [7] and has been first formulated by Corkum [8]: Under the action of strong laser fields on the atom, a wave packet is formed each time the laser field passes its maximum value. Within the next laser period there is a probability that the electron having a high kinetic energy returns to the ion. The energy of electrons, which do return back to the ion, is easily calculated from the classical electron trajectory in the laser field. For the maximum energy, one obtains $E_{\max} \approx 3.2U_p$, where U_p is the laser ponderomotive potential. Reencountering the ion, the electron radiates a burst of x rays with energy up to $\hbar\omega_c = 3.2U_p + I_p$, where I_p is the ionization potential. The general shape of the high-harmonics spectra contains a relatively fast drop at the lower harmonic numbers and a plateau at higher frequencies [9]. The plateau has a sharp cutoff at $\hbar\omega_c$. The value $\hbar\omega_c$ has been confirmed in numerous experiments [10–14] and numerical simulations [15–20].

From the mechanism of electron-ion reencounter, one expects that the high harmonics are phase locked and emerge in the form of ASPs. If the laser pulse is many oscillations long, a train of ASP is produced [12]. When the laser pulse duration is comparable to its period, then solitary attosecond pulses can be generated by the strongest swing of the laser electric field [1,13,17].

In the present paper, we simulate laser-atom interactions by direct numerical solution of the time-dependent Schrödinger equation (TDSE). We show that the spectrum of high harmonics, Fig. 1, consists of three parts. First, there is a dip in the range between the laser fundamental and the atomic ionization potential I_p. We find little radiation in this frequency range. Then, a power-law spectrum establishes in the range from I_p down to the begin of the plateau(s). Here, the intensity of higher harmonics scales similar to $I_\omega \sim \omega^{-3.3\pm0.25}$. In the range of the highest harmonics, we observe one or several plateaus, each produced by a laser oscillation of the respective amplitude. This radiation is attributed to the Corkum returns [8] of electron wave packets to the atom.

We make a spectrotemporal analysis of the emitted radiation. Our numerical approach is similar to the experimental method used by the Vienna group [3], where a multilayer Mo/Si mirror has been employed to select x rays in a narrow frequency window close to the plateau cutoff. We use a numerical filter with the spectral width of 15 eV, Fig. 2. Varying the mean frequency of the filter, we plot the results in the (t, ω) plane, Fig. 3, and observe well-defined bows: At a given time, the atom radiates at a single specific resonant frequency. This frequency corresponds to an electron wave packet that returns back to the incompletely ionized atom and recombines with it.

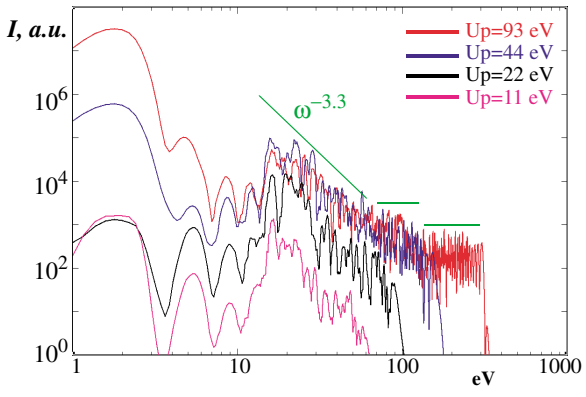

FIG. 1 (color). Spectral intensity (arbitrary units) of high harmonics for laser pulses with ponderomotive potentials $U_p =$ 11, 22, 44, and 93 eV.

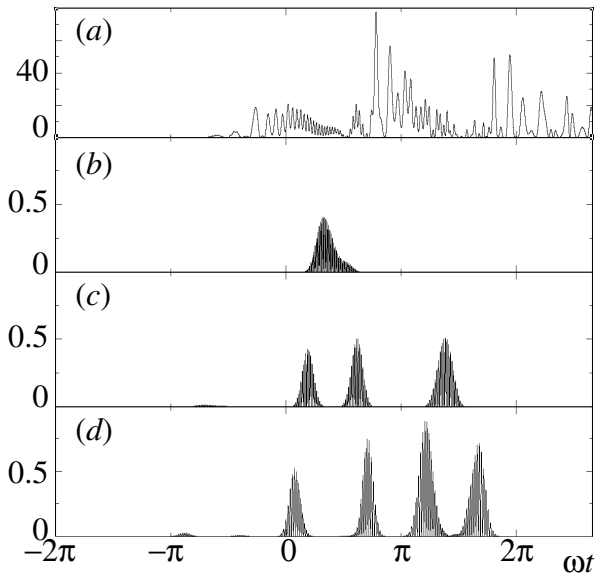

FIG. 2. Temporal profile of the radiation for the case $U_p = 44$ eV. (a) No filter applied: irregular pattern due to the lower harmonics. (b) Filter at 160 eV: a single ASP. (c) Filter at 130 eV: the ASP splits into two twins, and another ASP emerges 1/2 laser period later. (d) Filter at 100 eV: separation between the first twins increases; the second ASP splits as well. The filter width applied here is 15 eV.

We explain the strong resonant emission of photons with the energy $\hbar\omega = p^2/2m + I_p$ in terms of *stimulated recombination* (SR). The probability of this process is proportional to $|\langle\psi_0|\nabla|\psi_p\rangle|^2$, where ψ_p corresponds to a freed part of the electron in the continuum with the momentum p, and ψ_0 is a part of the same electron still remaining in the ground state.

We solve numerically the three-dimensional single-electron TDSE in cylindrical coordinates:

$$\mathbf{i}\,\partial_t\psi = -\frac{1}{2\rho}\partial_\rho(\rho\partial_\rho\psi) - \frac{1}{2}\partial_z^2\psi - \frac{1}{r}\psi - \varepsilon(t)z\psi\cos\omega t, \tag{1}$$

where $\rho = \sqrt{x^2 + y^2}$, $r = \sqrt{\rho^2 + z^2}$; $\varepsilon(t)$ is the laser field amplitude (envelope) and ω is the carrying frequency. Equation (1) is written in the usual Coulomb units [21]. In these units, the first Bohr radius is $r_0 = 1$, and the ground state energy level $E_0 = -1/2$. The critical field for the barrier-suppression ionization $\varepsilon_{\mathrm{BSI}} = 1/16$ [22].

Equation (1) had been widely studied earlier using grid methods [15,17], state-specific expansion approach [16], and other numerical methods [20]. It had been pointed out already in the first works on the topic [15,16] that the problems of accuracy and convergence are very important here. We exploit the standard semi-implicit finite difference scheme of Crank-Nicholson [23]. To apply the scheme smoothly everywhere in the simulation box, we integrate the Coulomb singularity analytically within the on-axis cells. We find converging results, when large enough simulation boxes with nonreflecting boundary conditions are used. The box size must be larger than the electron excursion length in the laser field. The sufficient accuracy is achieved by choosing a grid cell size small enough to resolve the highest electron energies. To calculate the emitted radiation, we use the current $\mathbf{j} = i\int_V \psi^*\nabla\psi\, d^3\mathbf{r}$, having in mind that $d_t\mathbf{j} = d_t^2\mathbf{d}$, where $\mathbf{d}$ is the dipole momentum.

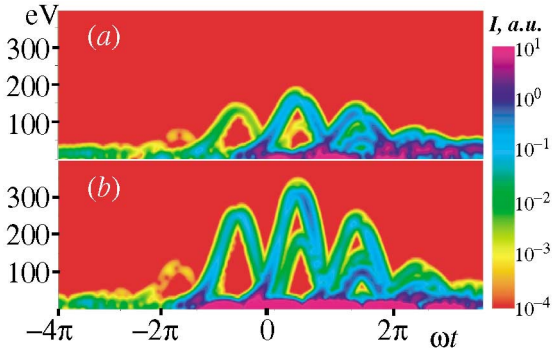

FIG. 3 (color). Spectral intensity (arbitrary units) vs time in TDSE simulations: (a) $U_p = 44$ eV; (b) $U_p = 93$ eV.

A number of simulations for a wide range of laser intensities and different ratios of $I_p/\hbar\omega_0$ have been made. In this paper, we restrict ourselves to the case $\omega = 0.04$, giving $I_p/\hbar\omega_0 = 12.5$. This set of parameters might correspond to a 750 nm laser pulse interacting with neon atoms ($I_p = 21.6$ eV). We emphasize that we solve a model single-electron problem and abstract from much more complicated multielectron dynamics of the real neon atom. The laser pulse has the Gaussian profile: $\varepsilon(t) = \varepsilon_0\exp(-t^2/\tau_L^2)$. The laser ponderomotive potential in eV expressed through parameters in the Coulomb units is $U_p(\mathrm{eV}) = 0.5I_p(\varepsilon_0/\omega)^2$. The corresponding laser intensity is $I = 1.07\times10^{13}U_p\lambda^{-2}\ \mathrm{W}\,\mu\mathrm{m}^2\,\mathrm{cm}^{-2}\,\mathrm{eV}^{-1}$.

Figure 1 shows high-harmonics spectra produced by laser pulses with $\omega\tau_L = 2.6\pi$ and ponderomotive potentials $U_{p(1,2,3,4)} = 11$, 22, 44, and 93 eV. The spectra are plotted in log-log scales. One clearly sees common features in the spectra. First, there is a gap between the laser fundamental and the atomic ground state frequencies. Then the spectra display power-law decay down to plateau regions. The straight line in Fig. 1 indicates the power-law slope −3.3. The plateaus end sharply at $3.2U_p + I_p$.

Looking at the radiation spectrum produced by a laser pulse with $U_p = 22$ eV, we mention that the spectral intensity at the plateau cutoff at 100 eV is only 1 order of magnitude smaller than the medium response at the laser fundamental. Thus, the generation of very high harmonics is energetically efficient and can be comparable with the refraction.

Figure 2(a) shows the radiation emitted by the atom as a function of time for the case $U_p = 44$ eV. We have zoomed the two laser periods around the pulse maximum. An irregular spiky pattern is seen here due to the lower harmonics. Clearly, there is no phase locking and no

regular ASPs can be recognized. We apply now a spectral filter to this radiation with the width of 15 eV and the central frequency located at the plateau cutoff 160 eV. The result is shown in Fig. 2(b). A clean single ASP appears. Its position roughly corresponds to the time when the laser electric field changes its sign. When we shift the filter down to 130 eV, the ASP splits into two twin ASPs around this time position and another ASP emerges about a half laser period later [Fig. 2(c)]. Shifting the filter further down to 100 eV, we see that the time delay between the first twin ASPs grows, and the second ASP splits into twins as well [Fig. 2(d)].

Using our filter, we have scanned the full range of frequencies and present the result as a spectrotemporal plot in the (t, ω) plane. Figure 3(a) shows the case $U_p = 44$, and Fig. 3(b) shows the case $U_p = 93$. Clear bow structures are seen in these plots. Evidently, the single ASP in Fig. 2(b) corresponds to the very top of the highest bow. The twins of ASPs in Figs. 2(c) and 2(d) are produced when we cut out parts of the descending arms of the bows. Going down in the mean frequency, additional ASPs emerge due to the lower bows.

The bows in Fig. 3 are produced when the electron moving along its classical trajectory returns to the atom with the kinetic energy $p^2/2m$ recombines and emits radiation resonantly at $p^2/2m + I_p$. The time t' when the electron has been extracted from the atom and the time t when it returns back are connected through the returns equation [24]:

$$A(t')(t - t') = \int_{t'}^{t} A(\tau)\, d\tau, \tag{2}$$

where A is the laser vector potential. The electron momentum at the return is $p = e[A(t) - A(t')]/c$. In Fig. 4(a), we plot the times t' as a function of t ($t = 0$ gives the pulse maximum). Evidently, several roots t' can be found for a single t, depending on how many oscillations the electron performs around the nucleus. Root branches, which belong to one half period of the laser field, are painted with the same color. Each of these roots t' gives one bow branch in the (t, ω) plane [Fig. 4(b)]. In the full TDSE simulation [Figs. 3(a) and 3(b)], we see only the most intense branches, corresponding to the electron extraction at large electric fields.

Now we ask the question: Why do we see mainly the resonant emission at $p^2/2m + I_p$? This emission can be explained only as the electron recombination to the atom. On the other hand, the probability to trap an electron flying with some 100 eV kinetic energy by an ion should be pretty small. Yet, this is the dominant process here. The reason is that the ground state is incompletely depleted. When the extracted electron wave packet returns back to the atom, it interferes with the ground state wave function. It is this interference that leads to the radiation emission and the enhanced electron recombination. We call this process *stimulated recombination*: The populated ground state *stimulates* the wave packet moving in the continuum to recombine.

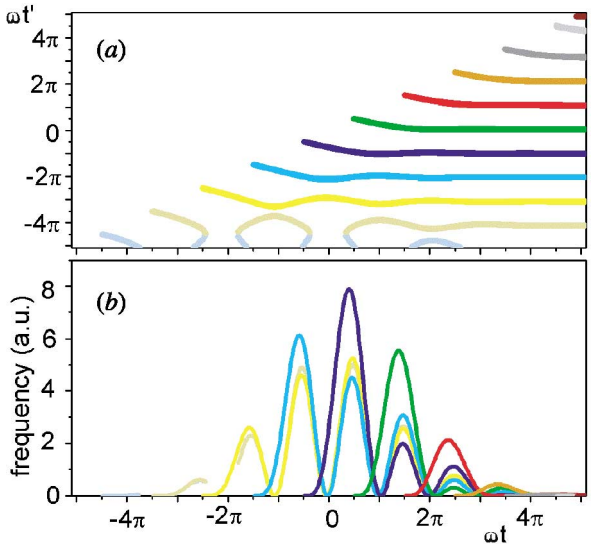

FIG. 4 (color). Solution of the returns Eq. (2): (a) roots t' for each t; (b) photon energy emitted at time t: $\hbar\omega(t) = 1/2[A(t) - A(t')]^2$. Compare Fig. 3.

Indeed, let us suppose that the ψ function of the electron can be represented as $\psi(t, \mathbf{r}) = \alpha_0\psi_0(t, \mathbf{r}) + \alpha_p\psi_p(t, \mathbf{r})$, where $\psi_0(t, \mathbf{r}) = (1/\sqrt{\pi r_0^3})\exp(iI_p t - r/r_0)$ is the ground state and $\psi_p(t, \mathbf{r}) = \exp[-i(p^2/2m)t + i\mathbf{pr}]$ is a continuum state with the momentum $\mathbf{p}$. We denote here r_0 the first Bohr radius. The constants $\alpha_{0,p}$ describe the population of these two states.

Calculating the current $\mathbf{j}$, we obtain

$$\mathbf{j} = \Im\left(2\alpha_0^*\alpha_p \int_V \psi_0^*\nabla\psi_p\, d^3\mathbf{r}\right) - i|\alpha_p|^2 \int_V \psi_p^*\nabla\psi_p d^3\mathbf{r}. \tag{3}$$

It is the cross term in Eq. (3) that oscillates at $p^2/2m + I_p$. Integrating, we get the following for the radiation source:

$$\mathbf{S}_{0p} = d_t\mathbf{j} = \frac{16\sqrt{\pi r_0^3}\mathbf{p}}{(1 + r_0^2p^2)^2}\left(I_p + \frac{p^2}{2m}\right) \times \Im\left\{\alpha_0^*\alpha_p \exp\left[-i\left(I_p + \frac{p^2}{2m}\right)t\right]\right\}. \tag{4}$$

Although the electron wavelength in the continuous spectrum is much smaller than r_0, this cross term is not exponentially small after the integration, because $\psi_0(t, \mathbf{r})$ has a cusp at $r = 0$ due to the Coulomb singularity.

For illustration, we have made TDSE simulations of a free electron wave packet traveling with the mean kinetic energy 50 eV and colliding with an ion. We consider two cases: (i) a completely ionized atom, $\alpha_0 = 0$, and (ii) an incompletely ionized atom with a part of the electron remaining in the ground state, $\alpha_0 = \alpha_p$. Simulation

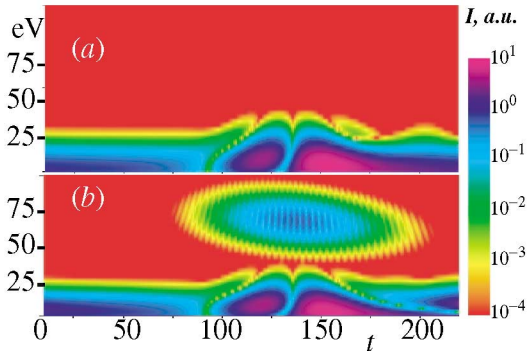

FIG. 5 (color). Spectral intensity (a.u.) vs time of radiation emitted in electron collision with (a) fully ionized atom (no SR). (b) Incompletely ionized atom (SR appears promptly). Mean energy of the electron wave packet is 50 eV.

results are shown in Figs. 5(a) and 5(b). In the naked ion case, Fig. 5(a), we observe little radiation. But, when the atom is incompletely ionized, Fig. 5(b), the resonant radiation due to the SR appears promptly.

Having clarified this issue, we may have a look at the phenomenology of ASP generation in intense laser-atom interactions. First, an electron wave packet is extracted from the atom at the time t' with probability $w_i(t')$. Then, the electron moves along its classical trajectory in the laser field and returns to the ion at the time t with momentum p. The diffraction reduces the amplitude of the electron wave packet by some factor $D(t, t')$. The diffraction is defined by the initial velocity spread of the electron at the ionization, and the latest experiments suggest ~ 5.6 A/fs for this value [25]. Finally, the SR takes place with the probability (4). The ASP amplitude according to this picture is $W_{\mathrm{ASP}} = w_i(t')D(t, t')|\mathbf{S}_{0p}|^2$.

In conclusion, we have studied high harmonic generation and attosecond pulse production from atoms in an intense laser field using *ab initio* numerical simulations. We directly solve the three-dimensional time-dependent Schrödinger equation. By spectrotemporal analysis of the emitted radiation, we obtain the characteristic "bow" structures in the (t, ω) plane. This radiation is produced when the freed electron oscillates in the laser field and returns back to the ion with a high kinetic energy. If the atom is in an incompletely ionized state, then the SR of the electron works and a resonant radiation is emitted at $I_p + p^2/2m$. One obtains attosecond pulses out of this radiation, when a finite bandwidth frequency filter is used. If the filter is applied at the very end of the plateau region in the spectrum, then the very top of the highest bow produces a single ASP. If the center frequency of the filter is down-shifted, then the filter cuts out parts of descending arms of the bows and twins of ASPs are generated per each half laser period.

The SR mechanism strongly relies on the incomplete ionization of the ground state. Thus, for the efficient generation of short-wavelength ASPs, one needs extremely short, few-cycle driving laser pulses [1].

We also find that intensity spectra of the high-harmonics display characteristic features in their general shape. First, there is a gap between the laser fundamental and the ionization potential of the atom. At higher frequencies, the harmonics show a power-law decay with the exponent -3.3 ± 0.25 down to the plateau region. The plateau ends abruptly at $3.2U_p + I_p$. In the simulation with $U_p = 22$ eV, we found that the radiation at the plateau cutoff is just 10 times less intense than the medium response at the laser fundamental (polarizability). This suggests that the generation of attosecond pulses is energetically quite efficient.

This work was supported in part by Alexander von Humboldt Foundation, DFG, and BMBF/Bonn. The simulations have been done at ZAM, Jülich.

[1] F. Krausz, Phys. World **14**, 41 (2001).
[2] M. Hentschel *et al.*, Nature (London) **414**, 509 (2001).
[3] R. Kleinberger *et al.*, Science **297**, 1144 (2002).
[4] M. Lewenstein, Science **297**, 1131 (2002).
[5] A. Baltuska *et al.*, Nature (London) **421**, 611 (2003).
[6] Ph. Bucksbaum, Nature (London) **421**, 593 (2003).
[7] A. L'Huillier and P. Balcou, Phys. Rev. Lett. **70**, 774 (1993).
[8] P. B. Corkum, Phys. Rev. Lett. **71**, 1994 (1993).
[9] N. Lewenstein, P. Balcou, M. Y. Ivanov, A. L'Huillier, and P. B. Corkum, Phys. Rev. A **49**, 2117 (1994).
[10] Ch. Spielmann *et al.*, Science **278**, 661 (1997).
[11] M. Drescher *et al.*, Science **291**, 1923 (2001).
[12] P. M. Paul *et al.*, Science **292**, 1689 (2001).
[13] N. A. Papadogiannis, B. Witzel, C. Kalpouzos, and D. Charalambidis, Phys. Rev. Lett. **83**, 4289 (1999).
[14] G. G. Paulus *et al.*, Nature (London) **414**, 182 (2001).
[15] J. L. Krause, K. J. Schafer, and K. C. Kulander, Phys. Rev. A **45**, 4998 (1992).
[16] S. Dionissopoulou, Th. Mercouris, and C. A. Nicolaides, J. Phys. B **29**, 4787 (1996).
[17] I. P. Christov, M. M. Murnane, and H. C. Kapteyn, Phys. Rev. Lett. **78**, 1251 (1997).
[18] G. G. Paulus *et al.*, Phys. Rev. Lett. **84**, 3791 (2000).
[19] M. W. Walser, C. H. Keitel, A. Scrinzi, and T. Brabec, Phys. Rev. Lett. **85**, 5082 (2000).
[20] N. Milosevic, A. Scrinzi, and T. Brabec, Phys. Rev. Lett. **88**, 093905 (2002).
[21] L. D. Landau and E. M. Lifshitz, *Quantum Mechanics* (Pergamon, Oxford, 1974), p. 369.
[22] S. Augst, D. D. Meyerhofer, D. Strickland, and S. L. Chin, J. Opt. Soc. Am. B **8**, 858 (1991).
[23] D. Potter, *Computational Physics* (Wiley, New York, 1977), p. 304.
[24] G. G. Paulus, W. Becker, and H. Walther, Phys. Rev. A **52**, 4043 (1995).
[25] H. Niikura, F. Legare, R. Hasbani, M. Y. Ivanov, D. M. Villeneuve, and P. B. Corkum, Nature (London) **417**, 917 (2002).